Supporting Information

Oxygen vacancy on Nb_2O_5 enhanced the performance of H_2O_2 electrosynthesis from O_2 reduction

Xiaoge Peng,‡ Shijie Zhang,‡ Zhikang Bao, Lei Ding, Guoliang Wang, Yizhen Shao, Zaixiang Xu, Wenkai Ji, Ge Feng, Shibin Wang, Xing Zhong, Jianguo Wang*

a. Institute of Industrial Catalysis, College of Chemical Engineering, State Key Laboratory Breeding Base of Green-Chemical Synthesis
Technology, Zhejiang University of Technology, Hangzhou 310032, Zhejiang, China.

‡ X.G. Peng and S.J. Zhang contribute to this work equally.

Corresponding Author

jgw@zjut.edu.cn (Jianguo Wang).

Contents:

Supplementary Experimental section

Supplementary Results

2. Experimental section

1. Materials Synthesis

Niobium Pentoxide (Nb_2O_5, Macklin, AR 99.9%), Nafion solution (DuPont), Cerium Sulfate ($Ce(SO_4)_2$, Aladdin, AR 98%), sulfuric acid (H_2SO_4, Lingfeng Chemical Reagent Co., Ltd, AR 99.9%), Potassium hydroxide (KOH, Sinopharm Chemical Reagent Co., Ltd, AR 99.5%), Ethanol (CH_3OH, Sinopharm Chemical Reagent Co., Ltd, AR 99.5%), deionized water (DI, Millipore 18.2 MΩ cm^{-1}), N_2 gas (99.99%), H_2 gas (99.99%) were used without further purification.

The commercial Nb_2O_5 powder was heated to 100, 200, 300, 400 and 500 °C at a heating rate of 5 °C min^{-1} under H_2 atmosphere and maintained 2 h. Subsequently, the samples were cooled down to room temperature under N_2 atmosphere. The as-fabricated sample was labelled as H-T (T is 100, 200, 300, 400 and 500 °C).

2. Characterization.

Scanning electron microscopy (SEM) inspections were conducted on a Hitachi FE-SEM S-4700 at 15 kV. Transmission electron microscope (TEM) images were conducted by Tecnai G2F30S−Twin operated at 300 kV. Power X-ray diffractometer (XRD) was recorded with a PANalytical X'Pert PRO powder diffractometer using Cu Kα radiation (λ = 0.1541 nm). X-ray photoelectron spectroscopy (XPS) measurement was performed on Thermo Scientific K-Alpha spectrometer with Al Kα radiation (hv = 1486.6 eV), calibration of the binding energies was done using the adventitious C 1 s peak at 284.8 eV. Electron spin resonance (ESR) was performed on Bruker EMX-plus. UV-vis was done on MICROSOLA equipment. Raman spectra was measured with a spectrometer (WITec alpha300R) using 488 nm excitation. photoluminescence (PL) spectroscopy was performed on the FLS980 with an excitation laser at 375 nm in the wavelength range of 400-700 nm at room temperature.

3. Electrochemical Measurements.

The ORR measurement was performed in O_2-saturated 0.1 M KOH solution, and the RRDE rotating rate of 1600 rpm. The three-electrode system: the drop-cast is used as the working electrode, the platinum (Pt) wire and saturated calomel electrode (Hg/Hg_2Cl_2) are used as the counter electrode and reference electrode, respectively. All reported potential is referred to as the reversible hydrogen electrode (RHE), which is calculated using the eq 1:

$$\mathrm{E(RHE)} = \mathrm{E(SCE)} + 0.0591 \times \mathrm{pH} + 0.241\ \mathrm{V} \quad (1)$$

The performance measurement of ORR was implemented, typically, the as-prepared catalyst (4.0 mg) and 5 wt.% Nafion solution (100 μL) were mixed in 900 μL ethanol solution followed by 0.5 h bath sonication to obtain a homogeneous ink. Then, the 5 μL as-prepared catalyst ink (5 μL) was dropwise to the disk-electrode of the RRDE (0.1256 cm^2 glassy carbon (GC) disk area, 0.1884 cm^2 Pt ring area) electrode and dried under the heating lamp. Linear sweep voltammetry (LSV) and

cyclic voltammetry (CV) were carried out at the scan rate of 50 mV s^{-1} and 10 mV s^{-1}, respectively, and O_2 flow rate of 30 mL min^{-1}. The H_2O_2 selectivity and electron transfer number (n) was calculated using the following eq 2 and eq 3, respectively. Where I_d is the disk current, I_r is the ring current and N is the collection efficiency.[1]

$$H_2O_2\ \% = \frac{Ir/N}{Ir/N + Id} \times 200\% \ (2)$$

$$n = 4 \times \frac{Id}{Ir/N + Id} \ (3)$$

The collection efficiency (N) was conducted as follow: 0.1 M KOH and 10 mM $K_3Fe(CN)_6$ as electrolyte on a blank RRDE electrode, where Fe^{3+} to generated Fe^{2+} on the disk electrode, subsequently was oxidated to Fe^{3+} on the ring electrode, the process only one-electron reaction to obtain the ring electrode collection efficiency.[2] [3, 4] Typically, RRDE voltammogram is recorded by performing LSV with different rotation rate (400, 625, 900, 1225, 1600, 2025 and 2500 rpm), and the potential range from 1.2 V to 0 V at the scan rate of 10 mV s^{-1}. Meanwhile, the ring potential is held at 1.30 V. The collection efficiency (N) of RRDE is calculated using the eq 4.[2]

$$N = \frac{Ir}{Id} \ (4)$$

The corresponding faradaic efficiency of RRDE can be obtained by eq 5:

$$\text{faradaic efficiency}\ (\%) = \frac{Ir/N}{Id} \times 100 \ (5)$$

4. The measurement of yield.

The homemade electrolytic cell includes the cathode and anode chamber, the 0.1 M KOH solution as electrolyte and the nafion 117 membrane is clamped between the middle of the two chambers. The hydrophobic gas diffusion layer (GDL) coating the catalyst powers be used the cathode, the anode coated with the Ir-Ta. To improve oxygen utilization, oxygen cavity at the bottom of the cathode chamber was set. The electrocatalyst is loaded on the GDL, where the whole lay out O_2.

The concentration of H_2O_2 is determined by a colorimetry.[5] Note, the production of H_2O_2 are accumulated during the ORR process. The detail of this method could be described as follows: As-prepared 50 μL solution was added into the 2 mL 10 Mm ($Ce(SO_4)_2$). The yellow Ce^{4+} is oxidized by H_2O_2 to colorless Ce^{3+} (eq 6). Subsequently, absorbance of the mixed solution is measured at UV-vis technology (λ = 316 nm), and the H_2O_2 concentration is identified by the standard curve.

$$2Ce^{4+} + H_2O_2 \rightarrow 2Ce^{3+} + O_2 + 2H^+ \ (6)$$

The corresponding faradaic efficiency of H_2O_2 production can be obtained by eq 7:

$$\text{faradaic efficiency}\ (\%) = 100 \times \frac{2 \times C \times V \times F}{Q} \ (7)$$

where C is the produced H_2O_2 concentration (mol L^{-1}), V is the volume of electrolyte (L), F is the faraday constant (96485 C mol^{-1}), Q is the passed charge amount (C).

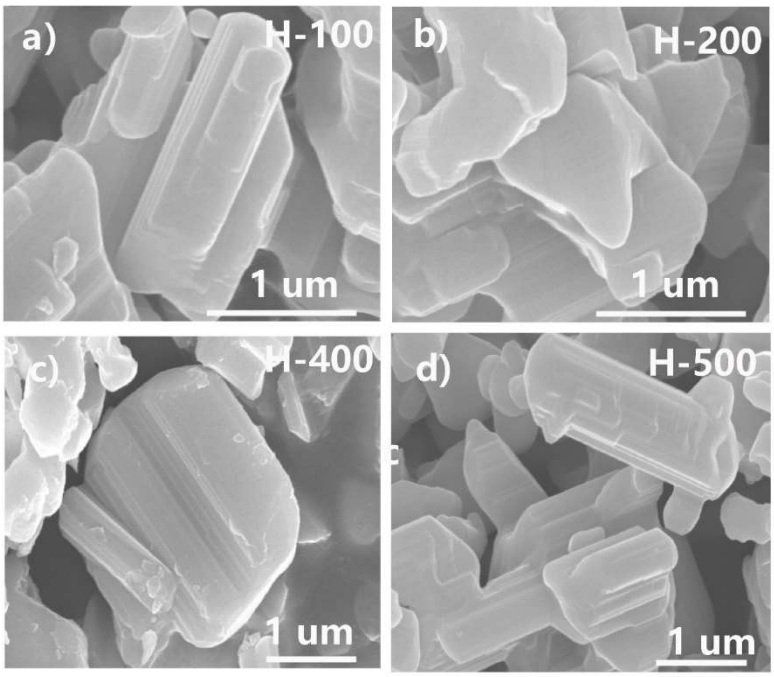

Figure S1. The SEM images of H-Nb_2O_5 materials were prepared at different temperatures. a) H-100. b) H-200. c) H-400. d) H-500.

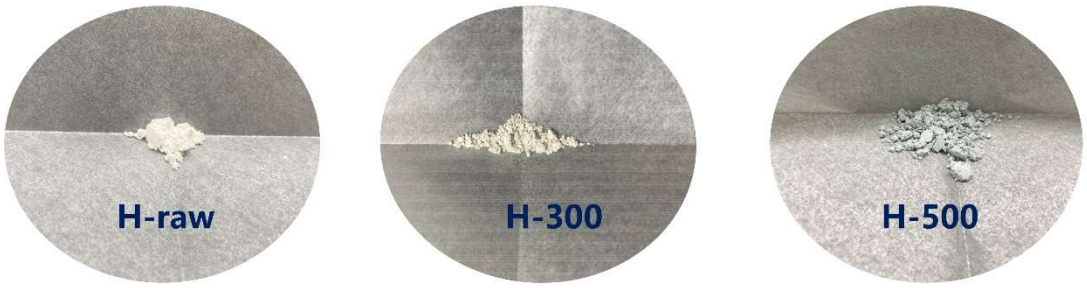

Figure S2. The catalyst power of Nb_2O_5 annealing at different temperatures. a) the pristine Nb_2O_5. b) annealing at 300 °C. c) annealing at 500 °C.

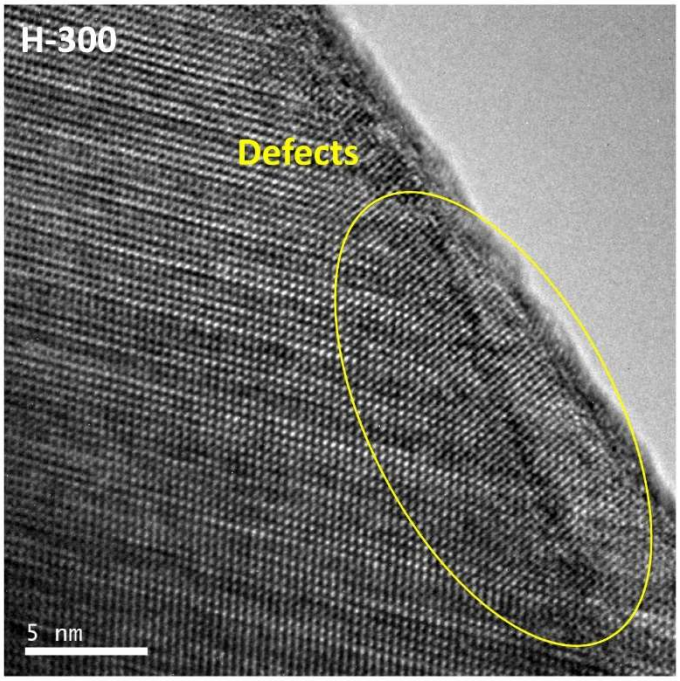

Figure S3. The TEM images of H-300 material (the yellow circle highlights the disorder area).

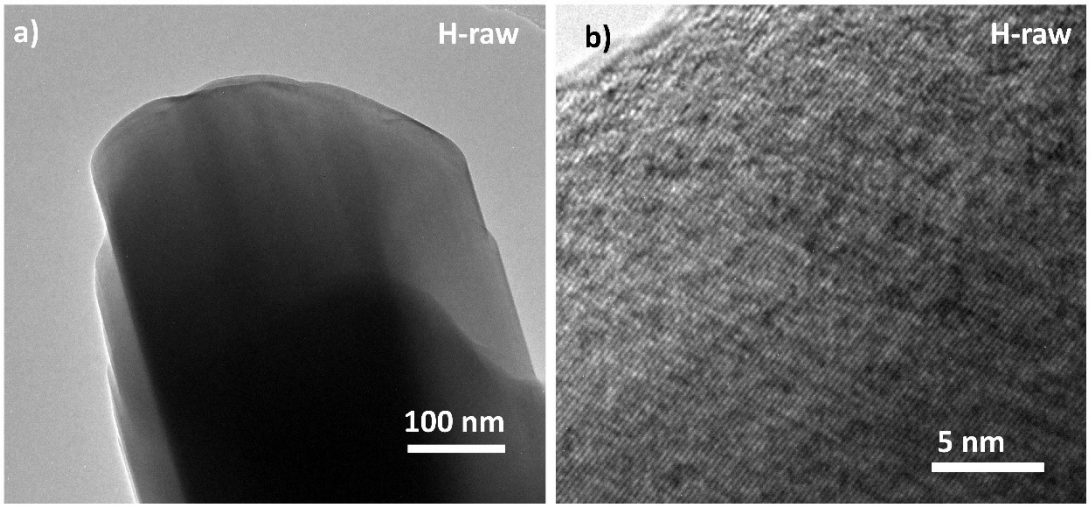

Figure S4. The TEM images of H-raw. a) at 100 nm. b) at 5 nm.

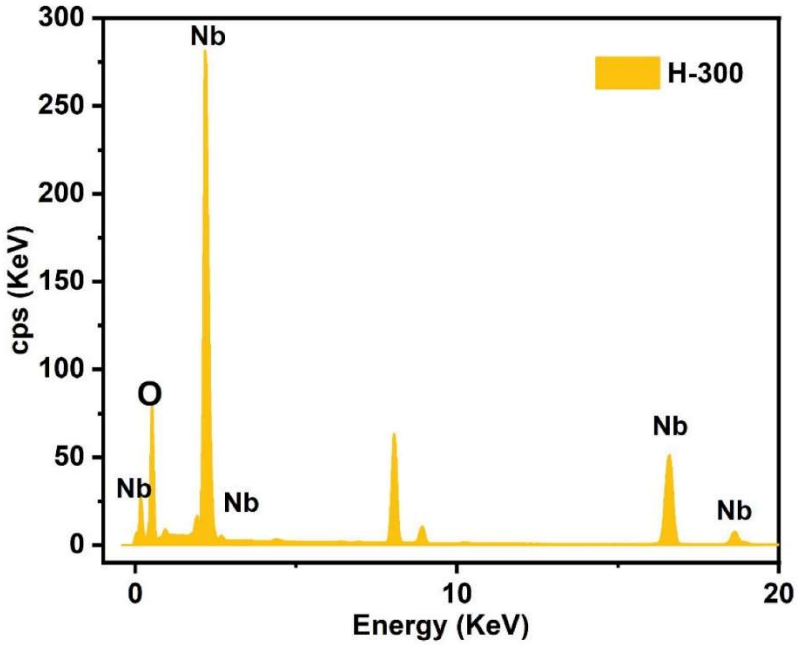

Figure S5. The EDS energy spectrum analysis results of H-300.

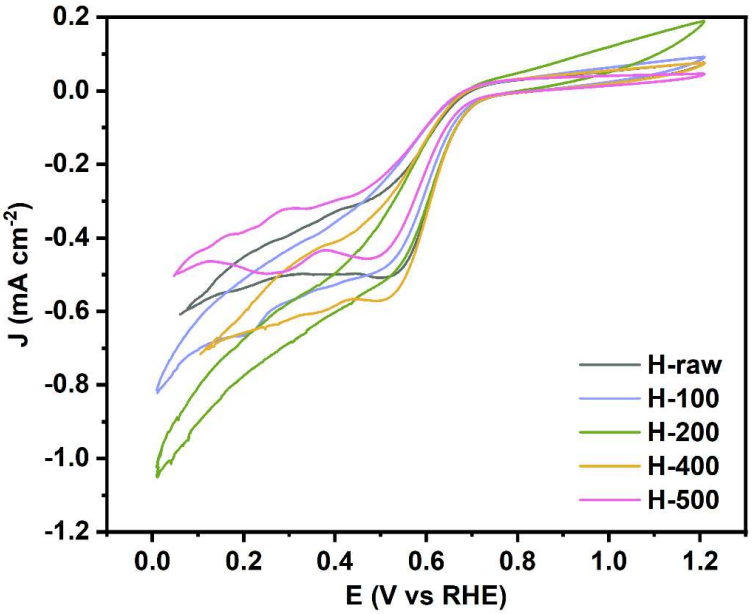

Figure S6. The CV of the H-raw, H-100, H-200, H-400 and H-500.

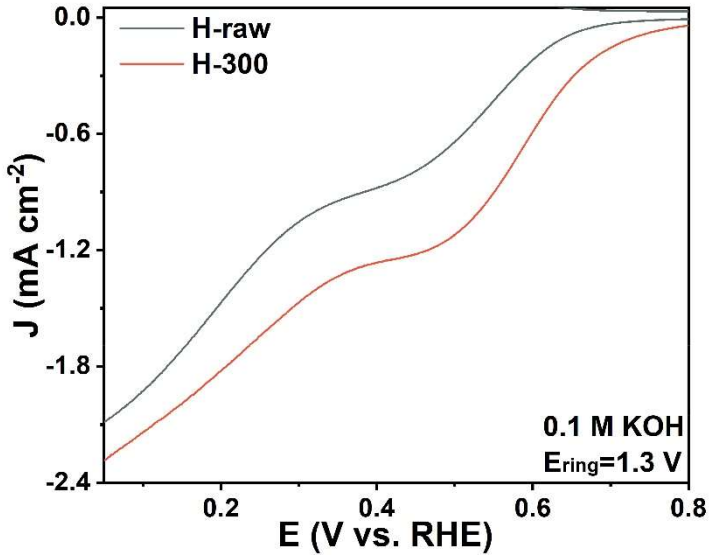

Figure S7. The LSV of the H-raw and H-300.

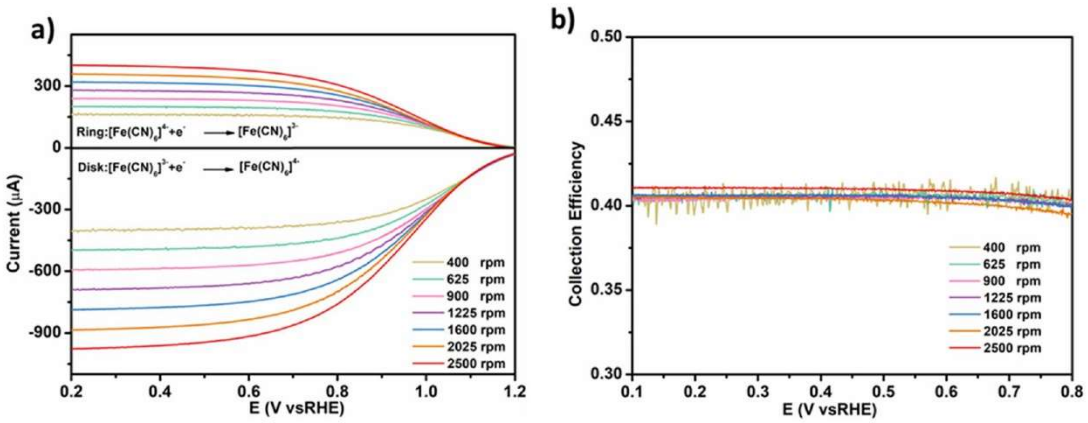

Figure S8. Measurement of the collection efficiency of the blank RRDE in Ar-saturated 0.1 M KOH dissolved with 10 mM of $K_3[Fe(CN)_6]$. a) RRDE voltammograms recorded at different rotation rates by performing LSV on the disk from 1.2 to 0 V_{RHE} at 10 mV/s while holding the ring potential at 1.50 V_{RHE}. b) the corresponding collection efficiency of RRDE voltammograms as a function of the potential. All potentials in this figure are presented without i_R-correction.

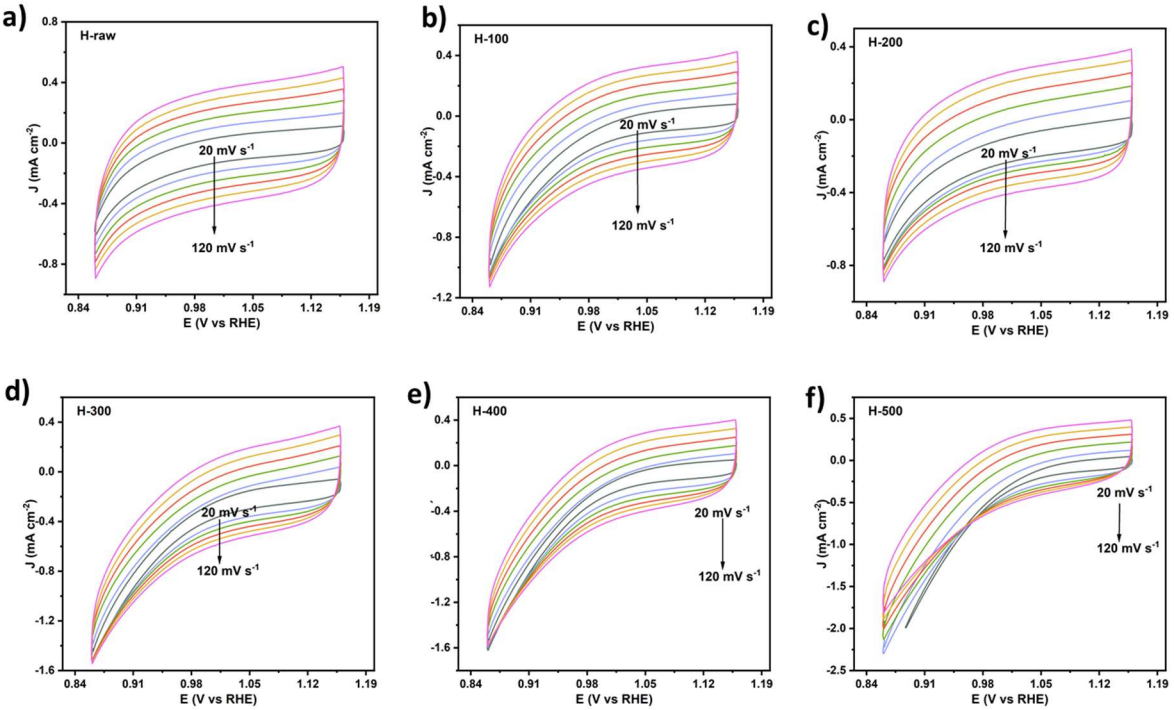

Figure S9. The ECSA analysis of H-T catalysts measured in 0.1 M KOH at different scan rate (20, 40, 60, 80, 100 and 120 mV s^{-1}).

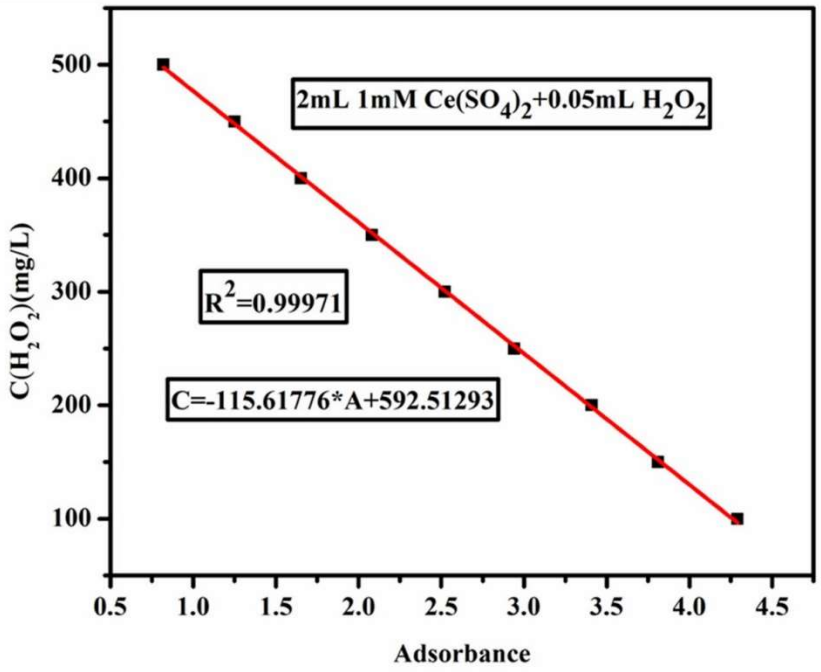

Figure S10. The calibration curve of $Ce(SO_4)_2$ solution and the standard curve of its reaction with hydrogen peroxide**.**

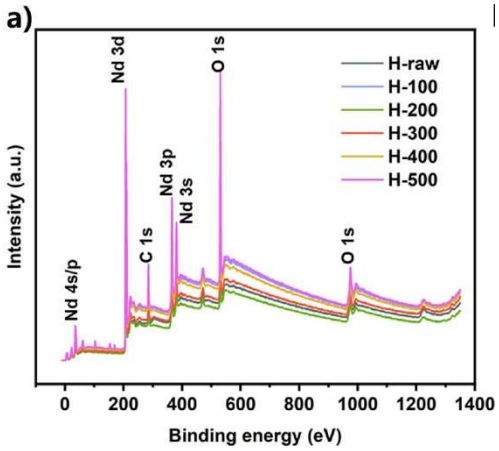

Figure S11. The XPS of H-T catalysts Full survey spectra.

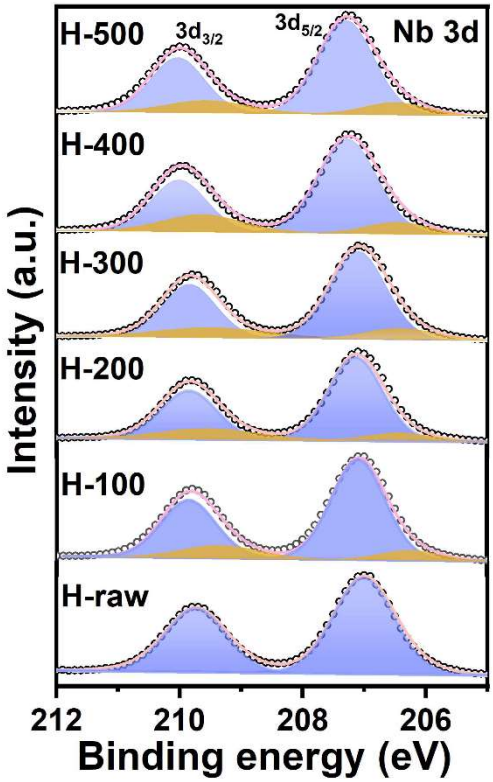

Figure S12. The Nb 3d XPS spectra of H-T catalysts.

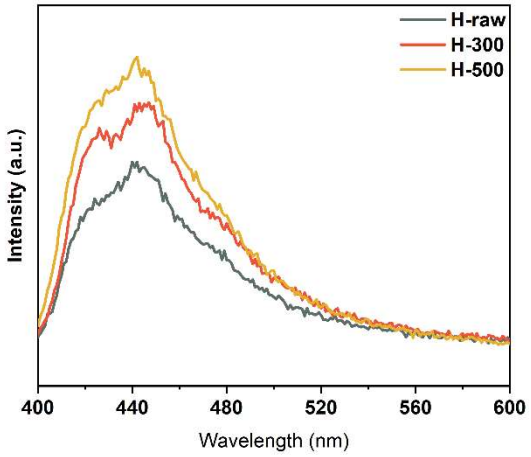

Figure S13. The photoluminescence (PL) spectroscope of H-raw, H-300 and H- catalysts.

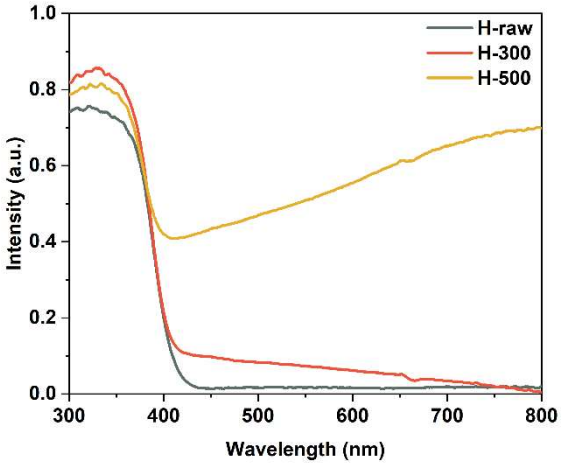

Figure S14. The UV-vis DSR spectroscope of H-raw, H-300 and H- catalysts.

Reference

1 C. Xia, J. Y. Kim and H. Wang, *Nat. Catal*, 2020, **3**, 605-607.

2 B. Q. Li, C. X. Zhao, J. N. Liu and Q. Zhang, *Adv Mater*, 2019, **31**, e1808173.

3 Z. Pei, J. Gu, Y. Wang, Z. Tang, Z. Liu, Y. Huang, Y. Huang, J. Zhao, Z. Chen and C. Zhi, *ACS Nano*, 2017, **11**, 6004-6014.

4 W. R. P. Barros, P. C. Franco, J. R. Steter, R. S. Rocha and M. R. V. Lanza, *J. Electroanal. Chem*, 2014, **722-723**, 46-53.

5 Z. Lu, G. Chen, S. Siahrostami, Z. Chen, K. Liu, J. Xie, L. Liao, T. Wu, D. Lin, Y. Liu, T. F. Jaramillo, J. K. Nørskov and Y. Cui, *Nat. Catal*, 2018, **1**, 156-162.